Numerical study of hydrogen dispersion in a fuel cell vehicle under the effect of ambient wind

Xing Yu [a,b], *Changjian Wang* [a,b,*], *Qize He* [c]

[a] *School of Civil Engineering, Hefei University of Technology, Hefei, Anhui 230009, China*
[b] *Anhui International Joint Research Center on Hydrogen Safety, Hefei, 230009, China*
[c] *Shanghai Fire Research Institute of MEM, 601 South Zhongshan 2nd Road, Shanghai, 200032, China*

ARTICLE INFO

ABSTRACT

In the rescue of hydrogen-fueled vehicle accidents, once accidental leakage occurs and hydrogen enters the cabin, the relatively closed environment of the vehicle is prone to hydrogen accumulation. Excessive hydrogen concentration inside the vehicle cabin may cause suffocation death of injured passengers and rescue crews, or explosion risk. Based on hydrogen fuel cell vehicle (HFCV) with hydrogen storage pressure 70 MPa, four different scenarios (i. with opened sunroof, ii. opened door windows, iii. opened sunroof and door windows and iv. opened sunroof, door windows and rear windshield) under the condition of accidental leakage were simulated using computational fluid dynamics (CFD) tools. The hydrogen concentration inside the vehicle and the distribution of flammable area (>4% hydrogen mole fraction) were analyzed, considering the effect of ambient wind. The results show that in the case of convection between interior and exterior of the vehicle via the sunroof, door windows or rear windshield, the distribution of hydrogen inside the vehicle is strongly affected by the ambient wind speed. In the least risk case, ambient wind can reduce the hydrogen mole fraction in the front of the vehicle to less than 4%, however the rear of the vehicle is always within flammable risk.

Introduction

Hydrogen is considered as one of the most potential clean energy sources in the future. Hydrogen used as an energy source in transportation system presents significant advantages over traditional fossil fuels, such as no harmful tail gas release, lower noise and higher efficiency.

In recent years, fuel cell vehicles have made great breakthroughs with hydrogen as fuel. Hydrogen in the fuel cell car Mirai manufactured by Toyota Motor Corporation is provided by two 70 MPa storage tanks placed in the rear part of the car.

Mirai supports a mileage of 700 km and the refueling process only takes about 3—5 min [1]. With the development of hydrogen storage technology, the performance of HFCV may be further improved.

However, HFCV still faces some problems, of which safety is the most significant due to the wide flammability, low ignition energy and great propensity to leak of hydrogen [2]. Once hydrogen leakage occurs, since it has the smallest molecular weight in all gases, high buoyancy and the jet velocity result in its quick dispersion in the vehicle and the formation of the flammable mixtures with air. If the hydrogen concentration reaches the flammability limit (4%—75% hydrogen

volume fraction) [3], serious explosion may occur after accidental ignition.

Some related safety analysis about HFCV have been performed in different scenarios using Computational Fluid Dynamics (CFD) tools, like in tunnels [4,5] and in an underground parking garage [6], etc. Moreover, some methods or measures for reducing hydrogen hazards have also been proposed. For example, Kožuh [7] developed a concept of hydrogen trap in road tunnel to prevent explosion caused by hydrogen leakage from HFCV after accidents. He modeled several vertical tubes on the ceiling of tunnel. According to numerical simulation by FLACS [8], hydrogen dissipates fast through the tubes because of high buoyancy and hydrogen concentration in tunnel drops rapidly. Liu and Christopher [9] simulated the dispersion of hydrogen around HFCV after accidental leakage at the bottom of the vehicle and placed a blower in front of the vehicle to decrease hydrogen concentration around it. The result shows that the blower can rapidly release hydrogen in air and causes H_2 concentration to be under the lowest explosion limit 4% within 15 s, except for a very small region under the vehicle. Tamura et al. [10] carried out a series of experiments to validate the effectiveness of the blower in decreasing hydrogen concentration around HFCV in case of hydrogen leakage and also got positive results. Salva et al. [11] studied the hydrogen dispersion inside a Santana 350 vehicle considering a leak located at the pipe joint. The internal pressure of hydrogen storage tank is 200 bar. They performed five scenarios with different inlet velocities of air conditioning system. The results show that air conditioning system combined with the exhaust vents in the back of vehicle can decrease internal hydrogen concentration and protect the front part of vehicle away from flammable risk.

With hydrogen-fueled vehicles gradually put into use, the quantity of related traffic accidents will inevitably increase gradually. In the rescue of hydrogen-fueled vehicle accidents, once accidental leakage occurs, hydrogen may disperse into the cabin and accumulate, which may cause injured passengers and rescue workers suffocation death or explosion risk. In the present study, a series of safety analyses were performed in the case of accidental hydrogen leakage. The car shell of BMW Series 1 saloon with two carbon fiber hydrogen tanks in the rear with storage pressure 70 MPa was employed. Note that 70 MPa is the highest hydrogen storage pressure for HFCVs in the market. Due to the high storage pressure, even a very small opening may cause a large amount of hydrogen leakage. When the sunroof or door windows of the vehicle are opened, the external air flows into the interior of the vehicle and may change the concentration and distribution of hydrogen inside. So, current numerical simulations were carried out based on the model of BMW Series 1 saloon, including four scenarios, opened sunroof, opened door windows, opened sunroof and door windows both and opened sunroof, door windows and rear windshield together.

Pseudo-source approach

If the direct numerical simulation is employed for hydrogen under-expanded jet, the computation is heavy and costs a lot of computer time [12]. Compromisingly, the pseudo-source approach, which was firstly proposed by Birch et al. [13], was employed in this paper. Even though small gap exists between pseudo-source approach and the direct numerical simulation [14—16], it can greatly reduce the computational complexity.

Some well-known pseudo-source approaches are proposed by Birch et al. (1984) [13], Birch et al. (1987) [17], Ewan et al. [18] and Schefer et al. [19]. The approach by Birch et al. (1984) [13] considers only the conservation of mass between jet orifice and pseudo-source with the assumption that the temperature at pseudo-source is equal to the atmospheric one. The approach by Birch et al. (1987) [17] considers the conservations of both mass and momentum and directly uses stagnation temperature as the one at pseudo-source. The approach by Ewan et al. [18] is similar to that by Birch et al. (1987) [17], but assumes that the temperature of pseudo-source equals to that of the actual jet orifice. The approach by Schefer et al. [19] takes the real gas properties into account and adopts Abel-Nobel equation of state to calculate the gas properties instead of the complex two-constant van der Waals equation and the Beattie-Bridgeman equation with five constants [20]. Other attempts also take into account the conservation of energy [21,22] or propose the location of the pseudo-source being after the Mach disk [23].

Considering the high storage pressure, the hydrogen behavior departs from an ideal gas. The approach by Schefer et al. [19] is adopted and the real-gas behavior of hydrogen can be adequately described through an Abel-Nobel equation of state [19].

$$P = \frac{\rho R_{H_2} T}{1 - b\rho} \tag{1}$$

where b is the co-volume constant with value 7.691×10^{-3} m³/kg for hydrogen and R_{H2} is the gas constant. Rearranging Eq. (1), the gas density of hydrogen stored in tanks, at temperature T_0 and pressure P_0, is given by

$$\rho_0 = \frac{P_0}{P_0 b + R_{H_2} T_0} \tag{2}$$

For fully turbulent jet [24], the characteristics of hydrogen release could be depicted by the Froude number which indicates the ratio of inertia to buoyant forces in Equation. 3. High Froude number (Fr > 1000) indicates that the flow is dominated by momentum and low Froude number (Fr < 10) indicates buoyancy dominant [25]. In turbulent buoyant jets, the region in the vicinity of the jet exit is dominated by momentum while in the far field is dominated by buoyancy. And an intermediate region is located between the two regions. The distance from the pseudo-source to the farthest momentum-dominated region could be described by Equation. 4 [26]:

$$Fr = \frac{\rho_j U_j^2}{g d_j |\rho_\infty - \rho_j|} \tag{3}$$

$$x_b = Fr^{-1/2} \left(\frac{\rho_j}{\rho_\infty}\right)^{-1/4} \left(\frac{x}{d_j}\right) \tag{4}$$

where d_j, ρ_j, U_j are diameter, density and velocity at the pseudo-source, ρ_∞ is atmospheric density, g is gravity acceleration, x is the distance between measuring point and pseudo-source and when $x_b < 0.53$ the flow is momentum-dominant.

The momentum dominant region of a round turbulent jet could be considered as self-similar region. The centerline velocity and sectional radius vary according to below equations [27]:

$$\frac{U(x)}{U_j} = \frac{B}{(x - x_0)/d_j} \tag{5}$$

$$r(x) = S(x - x_0) \tag{6}$$

where B = 5.8 and S = 0.094 are empirical constants, U(x) is centerline velocity, r(x) is half width of diffusion region, x_0 is the distance between pseudo-source and jet exit, and x is the distance between measuring point on centerline and jet exit.

Velocity and concentration decay validation

In order to ensure the accuracy of simulation, a set of experimental data of hydrogen jet was chosen to validate the simulation results. The jet exit was located 0.9 m away from the ground and jet orientation is horizontal. The experimental details could be found in Ref. [16], named HD22-24. The experimental data are presented in Table 1. In simulation, the storage pressure of 162 bar was selected as the initial one. The x value is 5.26 m, which renders all the measuring points are within the momentum dominant region.

In the present study, the open source CFD software OpenFOAM [28] was applied and two equations k-ε model was adopted in the turbulence calculation. The details of numerical set up were described as below:

- The stagnation temperature was set to 14.5 °C, equal to the ambient temperature [16].
- The pseudo-source approach proposed by Schefer et al. [19] was used.
- The 1st order resolution scheme was used for solving time terms while the 2nd order resolution scheme was applied to the discretization of convective and diffusive terms.

Fig. 1 presents the simulated and measured velocities and hydrogen mass fractions on the centerline. The simulation and experimental results are in reasonable agreement and the measured velocities and hydrogen mass fractions are slightly lower than the simulated data. So current numerical technology can be employed for the analysis of hydrogen dispersion inside a fuel cell vehicle.

Physical and numerical models

Physical model

In current study, HFCV models were established based on geometry of BMW series 1 saloon and two hydrogen tanks were installed in the rear part of vehicle. The overall size of the vehicle was approximately 4.30 m in length, 1.73 m in width and 1.43 m in height. Considering the small molecular weight and high buoyancy, hydrogen inside the vehicle is most likely to disperse quickly through the sunroof to the atmosphere. Thus, the vehicle model with opened sunroof was modeled as shown in Fig. 2a. In addition, considering the large area of door windows for hydrogen dispersion, the vehicle with opened door windows at both sides was also modeled as presented in Fig. 2b. It should be mentioned that the B-pillar between front and rear door windows was not considered, so the front and rear door windows at each side were merged into a whole. The vehicle model with opened sunroof and door windows at the same time was modeled as shown in Fig. 2c. Besides, considering that the rear windshield was located in the rear of the vehicle, it could be used as an emergency measure for hydrogen discharge. Thus, the vehicle model with opened sunroof, door windows and rear windshield was built as presented in Fig. 2d. The area of sunroof, two door windows and rear windshield was 0.228 m², 1.218 m² and 0.707 m², respectively.

Due to the complex structure of the vehicle, some necessary simplifications were made. Some internal components, like steering wheel, pedals and etc., were removed. Resultantly the remaining components inside the vehicle were mainly the seats, hydrogen storage tanks and connecting pipes.

The leaking point was located at the pipe joint of two storage tanks laid in the rear of vehicle, as highlighted in Fig. 3. Due to the required seals for the joint which may be damaged after long-term use, the possibility of leakage is higher than other areas during traffic accidents. For simplification, the direction of hydrogen leaking is set to be straight up. Normally for hydrogen fueled saloons, storage tanks are separated from the passenger compartment. In traffic accidents, considering the pipe joint and the partition between tanks and the passenger compartment may be damaged, hydrogen may leak into the passenger compartment.

Numerical model

In current study, the whole flow region considered in numerical simulation was a cuboid, with length 20 m, width 8 m and height 5 m. To simulate the ambient wind, air inlet

Table 1 — Experimental conditions.					
Test No.	Jet exit Diameter (mm)	Pressure (bar)	Flow rate (10^{-3} kg/s)	x (m)	Distance from jet exit (m)
HD 22-24	0.25	162.8	0.46	5.26	0.75
		160.4	0.45		1.5
		162.1	0.46		2.25
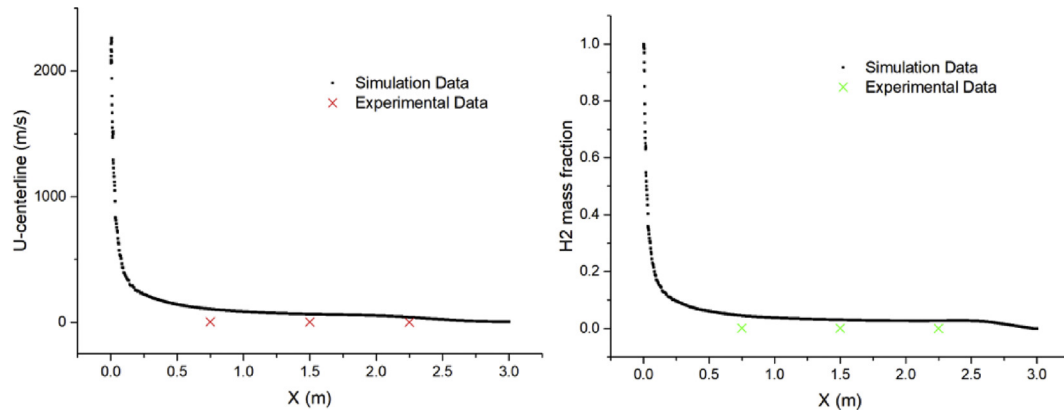
Fig. 1 – Centerline flow velocity (left) and hydrogen mass fraction (right) for test HD22-24.
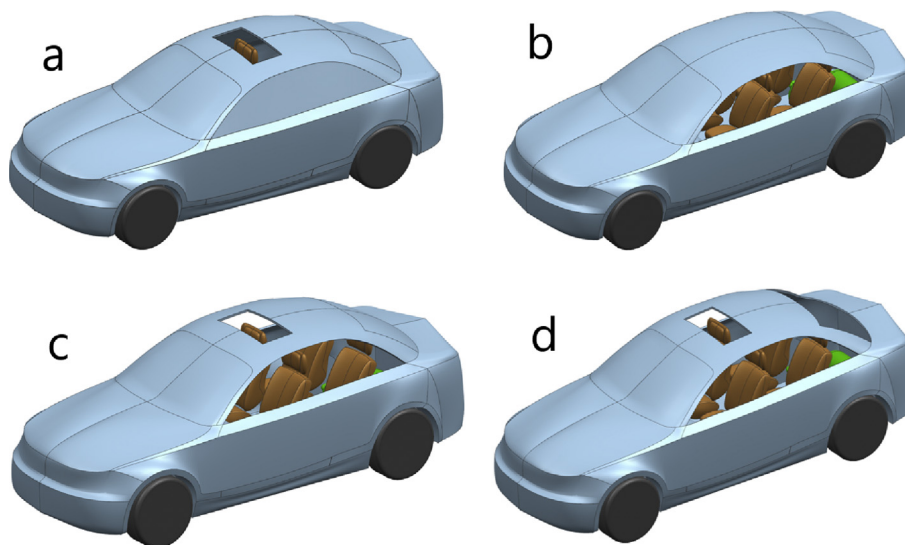
Fig. 2 – Geometry of BMW series 1 Saloon. (a) opening sunroof; (b) opening door windows of both sides; (c) opening sunroof and door windows both; (d) opening sunroof, door windows and rear windshield.

surface and air/hydrogen mixture outlet surface were designed as presented in Fig. 4. Considering the complex structure of vehicle, the region close to vehicle surfaces was meshed finely by tetrahedral cells while the outer region far from vehicle was meshed coarsely by hexahedron dominant cells to reduce the calculation time.
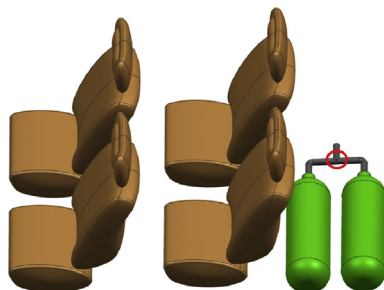
Fig. 3 – Internal components and leaking point.

Numerical set up

The boundary conditions for current analysis contained the hydrogen velocity-inlet, ambient wind velocity-inlet and pressure outlet, as shown in Fig. 4. Hydrogen leakage position was located at the pipe joint of two hydrogen storage tanks, and that the leakage diameter was assumed as 1 mm. The flow process between hydrogen storage tank and the orifice was considered as an isentropic expansion [29]. According to compressible flow theory, the leaking orifice was under choke flow condition due to high storage pressure of hydrogen, and therefore the hydrogen velocity at orifice would be sonic. After leaving the jet orifice, the expansion caused gas velocity to exceed the local sound speed, which causes the numerical simulation to be strongly nonlinear and extremely challenging.

The pseudo-diameter and related parameters are listed in Table 2. The hydrogen inlet has a pseudo-diameter 13.63 mm and inlet velocity 2226 m/s at 298.15 K and 1.0 atm. Due to the larger size of pseudo source compared to the leakage orifice,
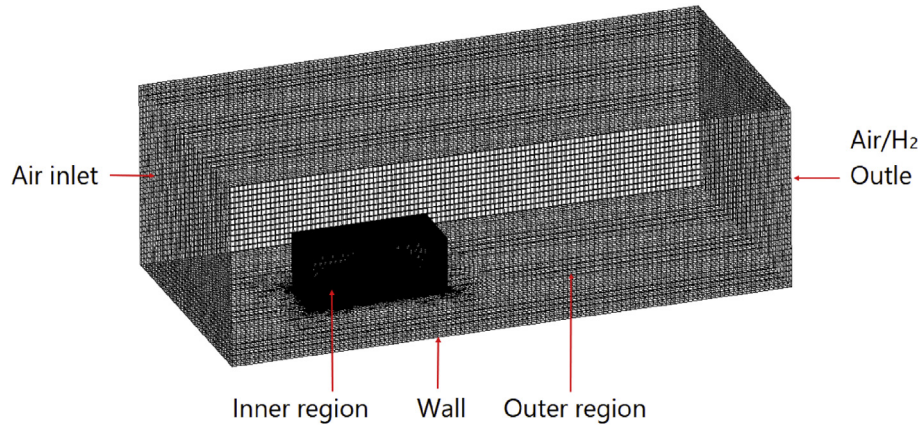
Fig. 4 – Superficial mesh of flow region.

the pseudo-source approach could effectively reduce the requirement of grids and the computing time.

In addition, 6 different ambient wind speeds, 20 km/h, 40 km/h, 60 km/h, 80 km/h, 100 km/h and 120 km/h were adopted in each scenario. Normally, the wind scales above level 6 (39—49 km/h) are not very common on land [30]. Considering large size blowers may be applied in the rescue of hydrogen-fueled vehicle accidents [9], which could produce much stronger winds than natural winds, a wide range of wind speeds were adopted in this study. The ambient wind direction was specified from the front of vehicle to the tail.

Taking all the variables into consideration, including 4 different vehicle geometries and 6 different wind speeds, the simulations of 24 scenarios were carried out in current study.

Grid independence study

To represent the distribution of hydrogen inside the vehicle, a sampling line from front to rear of the vehicle was chosen, as shown in Fig. 5. This line is on the middle plane of vehicle in the direction of length and the start point is in the front, near the control panel where electronic devices are installed. The length of the sampling line is 2.987 m.

In order to study the grid independence, 4 numerical tests were conducted using the scenario with opened door windows at wind speed 20 km/h. The element size of the outer region in Fig. 4 was set to 0.1 m and the inner region was meshed according to 4 different element size, 0.08 m, 0.05 m,
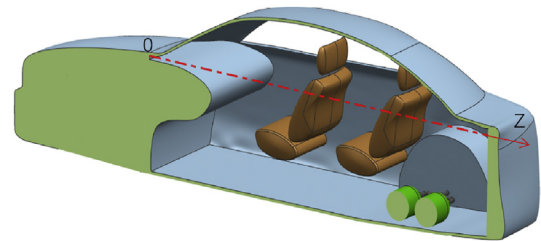
Fig. 5 – The sampling line to show hydrogen mole fraction inside the vehicle.

0.04 m and 0.035 m. The corresponding total element numbers are 1,919,863, 2,262,778, 2,785,147 and 3,350,053. As presented in Fig. 6, the abscissa values are positions on the sampling line and the ordinate values are the mole fractions of hydrogen. The results show that no significant difference of the hydrogen mole fraction could be seen with the mesh number larger than 2,785,147. Thus, the element size chosen in the present study is 0.1 m for outer region and 0.04 m for inner region.

Table 2 – Hydrogen inlet conditions.	
Jet direction (H-horizontal; V-vertical)	V
Orifice diameter (mm)	1
Tank pressure (bar absolute)	701
Tank temperature (K)	298.15
Ambient temperature (K)	298.15
Ambient pressure (bar absolute)	1
Pseudo conditions	
Diameter (mm)	13.63
Velocity (m/s)	2226
Temperature (K)	298.15
Pressure (bar absolute)	1
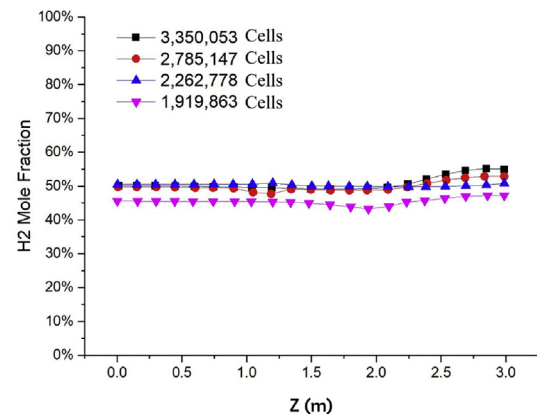
Fig. 6 – Hydrogen mole Fraction on sampling line for various cell sizes.

Results and discussion

Opened sunroof

For the scenarios with opened sunroof at different wind speeds, the hydrogen mole fractions on the sampling line are plotted in Fig. 7. When the wind speed is 20 km/h, hydrogen mole fraction below the sunroof is significantly lower than that in the front and rear parts of the vehicle. With the wind speed increasing, the hydrogen mole fraction on the whole sampling line generally present a declining trend and in the region below the sunroof drops rapidly. However, when the wind speed is higher than 80 km/h, high speed of the air outside the vehicle brings negative effects on the hydrogen dispersion in the vehicle and causes the hydrogen mole fraction on the sampling line to rise. As shown in Fig. 7, when the sunroof is opened with wind speed ranging from 20 km/h to
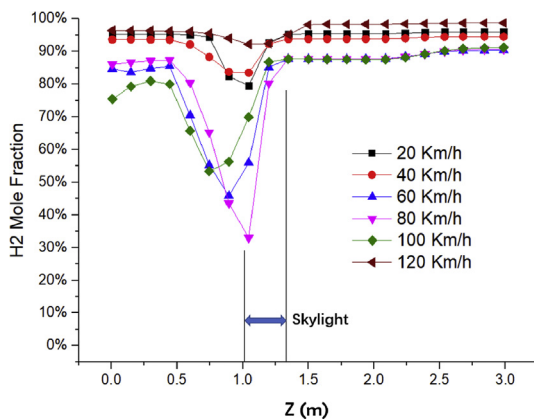
Fig. 7 – Hydrogen mole fractions on the sampling line for scenarios with opened sunroof.

120 km/h, the hydrogen mole fractions on the whole sampling line are always above the lower explosion limit of hydrogen.

In order to clearly display the regions with flammable risk, only areas with hydrogen mole fraction higher than 4% are visualized. It should be pointed out that even though the areas with hydrogen mole fraction over 75% are free from ignition risk, high concentration of hydrogen poses a potential security risk and low oxygen concentration may lead to asphyxia death. Thus, regions with hydrogen mole fraction ranging from 75% to 100% are also included in the hazardous area. Fig. 8 presents the regions with the flammable risk in red color for the scenarios with opened sunroof at different wind speeds. Although ambient winds could change hydrogen distribution and concentration inside the vehicle through the sunroof, due to excessive hydrogen leakage from the high-pressure storage tanks (0.027 kg/s), the whole interior of the vehicle is completely within flammable risk from 20 km/h to 120 km/h.

Opened door windows

For scenarios with opened door windows, hydrogen mole fractions on the sampling line are significantly lower than those in the case with opened sunroof at same wind speeds as presented in Fig. 9. When the wind is 20 km/h, hydrogen mole fraction on the sampling line is relatively uniform, approximate 50%. When the wind speed rises to 40 km/h, hydrogen mole fraction drops slightly to around 45%. With the increase of wind speed, the hydrogen mole fraction in the front of the vehicle drops sharply to below 4% and in the rear part of the vehicle remains at around 40%. However, when at 100 km/h, although no hydrogen exists in the front part of the vehicle, the hydrogen concentration in the rear begins to rise. At 120 km/h, the hydrogen mole fraction in the rear even exceeds that at 20 km/h, rising to about 70%.

Fig. 10 presents the regions with the flammable risk for the scenarios with opened door windows at both sides of the
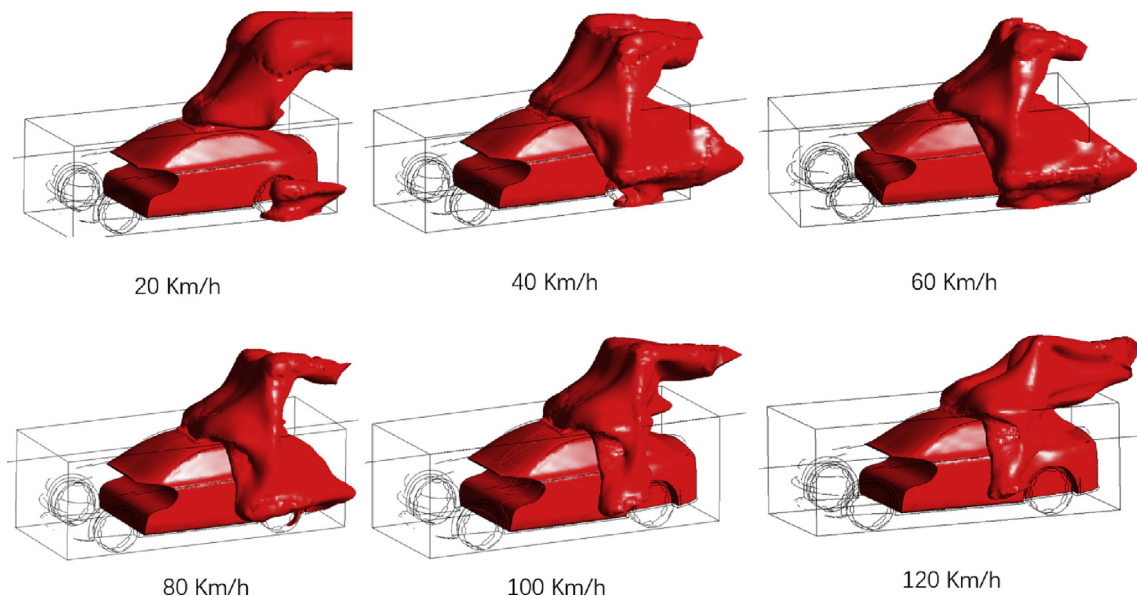
Fig. 8 – Region with flammable risk for scenarios with opened sunroof.
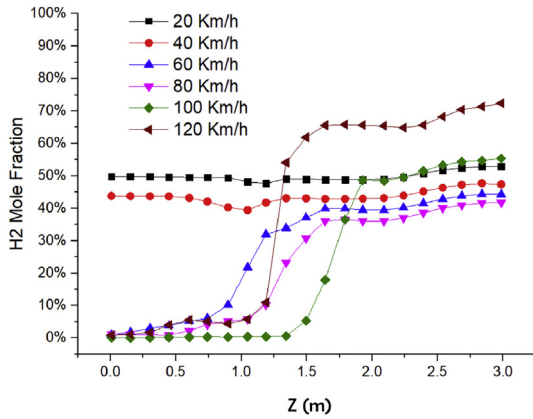
Fig. 9 — Hydrogen mole fractions on the sampling line for scenarios with opened door windows.
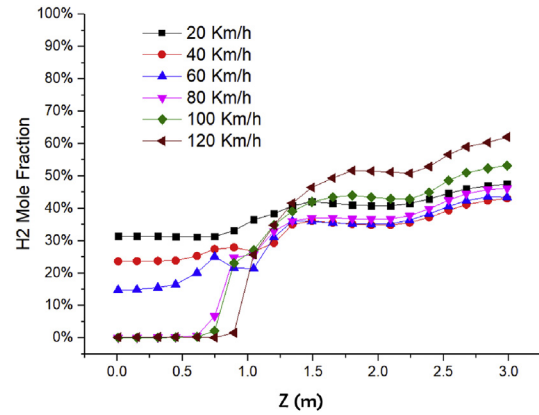
Fig. 11 — Hydrogen mole fractions on the sampling line for scenarios with opened sunroof and door windows.

vehicle. At 20 km/h, most of the internal region is flammable except for a small area near the doors. With the increase of wind speed, the flammable area of the front part of vehicle gradually decreases. At 100 km/h, the whole front area of the vehicle is free from flammable risk. However, as the ambient wind speed further increases to 120 km/h, hydrogen dispersion is blocked by the high velocity of the external air and most of the internal part of the vehicle are within the ignition risk again.

Opened sunroof and door windows

As presented in Fig. 11, while both the sunroof and the door windows are opened, the distribution of hydrogen mole fraction on the sampling line is similar to that when opening the door windows only, but the hydrogen concentration was slightly lower. At 20 km/h, hydrogen mole fraction in the front is approximately 30% while that in the rear is around 45%.

With the increase of wind speed, the hydrogen mole fraction in the front of the vehicle drops rapidly and in the rear part remains around 35%. When the wind speed reaches 80 km/h, hydrogen mole fraction of the front part on the sampling line drops to 0. However, when at 100 km/h, although hydrogen in the front part of the vehicle is completely discharged, the concentration in the rear rebounds. At 120 km/h, the hydrogen mole fraction in the rear even rises to about 60%.

Fig. 12 presents the regions with the flammable risk for scenarios with opened sunroof and door windows at the same time. With the increase of wind speed, the area with flammable risk gradually decreases to the rear of the vehicle. When the wind speed is accelerated to 120 km/h, the whole front area is free from ignition risk. Different from the scenarios with opened door windows only, the size of dangerous area has no rebound at 120 km/h. Generally, for scenarios with opened sunroof and door windows both, the size of safe region inside the vehicle is proportional to the wind speed.

20 Km/h   40 Km/h   60 Km/h

80 Km/h   100 Km/h   120 Km/h
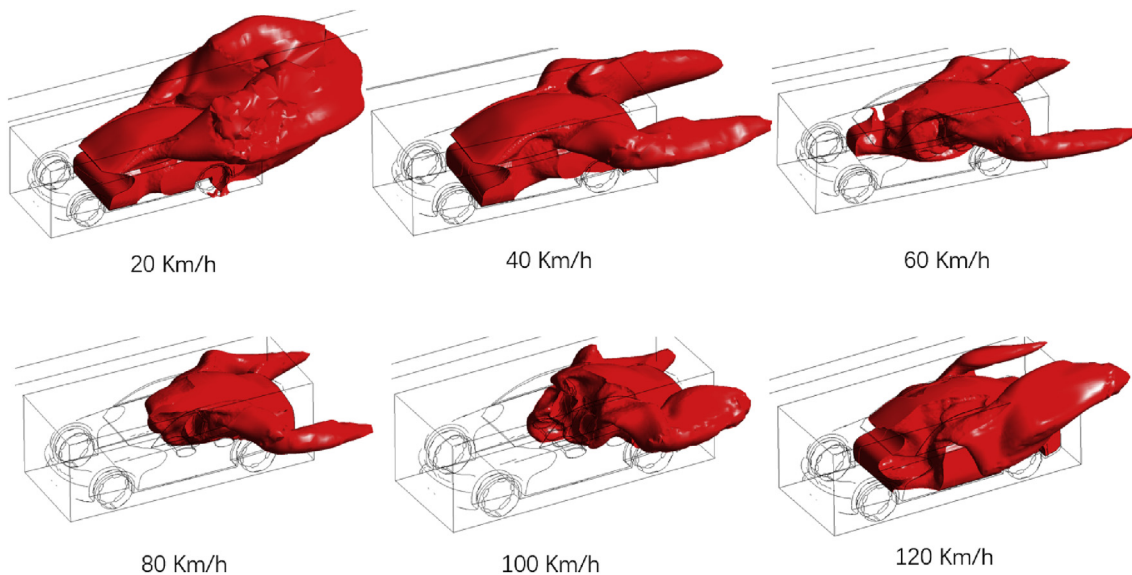
Fig. 10 — Region with flammable risk for scenarios with door windows.
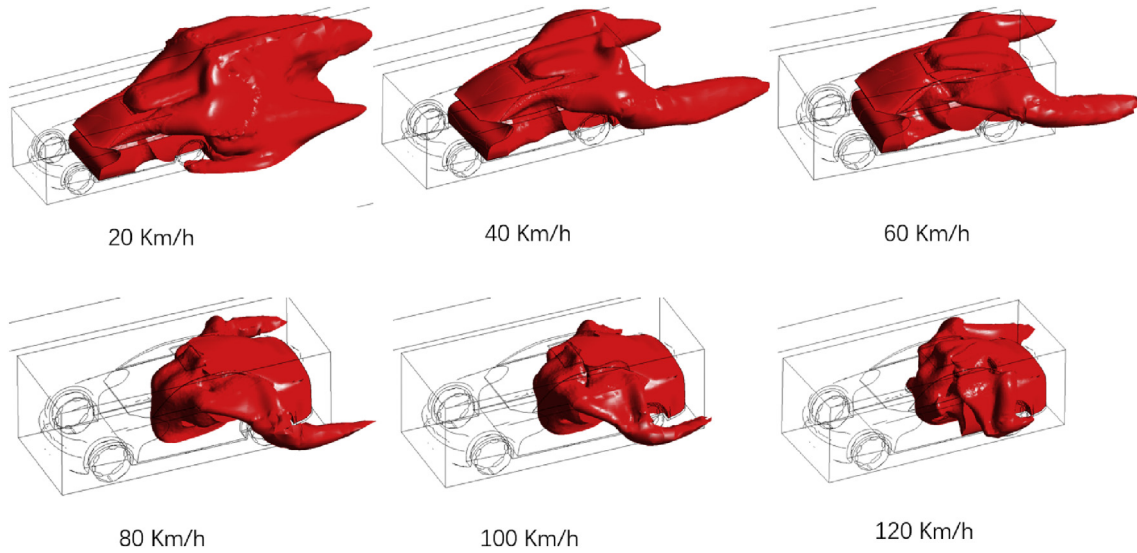
Fig. 12 — Region with flammable risk for scenarios with opened sunroof and door windows.
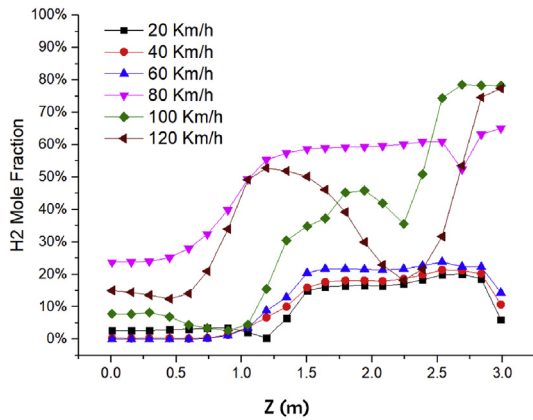
Fig. 13 — Hydrogen mole fractions on the sampling line for scenarios with opened sunroof, door windows and rear windshield.

Opened sunroof, door windows and rear windshield

Considering that the hydrogen storage tanks are installed in the rear of the vehicle, the hydrogen concentration in the rear of the vehicle is generally higher than that in the front of the vehicle. Thus, the opened rear windshield may have a great influence on hydrogen diffusion. For the scenarios with opened sunroof, door windows and rear windshield together, hydrogen mole fractions on the sampling line are presented in Fig. 13. Unlike previous scenarios, when the wind speed is low, the concentration of hydrogen is generally lower than that at high speed. From 20 km/h to 60 km/h, hydrogen mole fraction in the whole front part of the vehicle is under the lower explosion limit and in the rear remains at about 20%. From 80 km/h to 120 km/h, hydrogen mole fractions on the sampling line all exceed 4%.
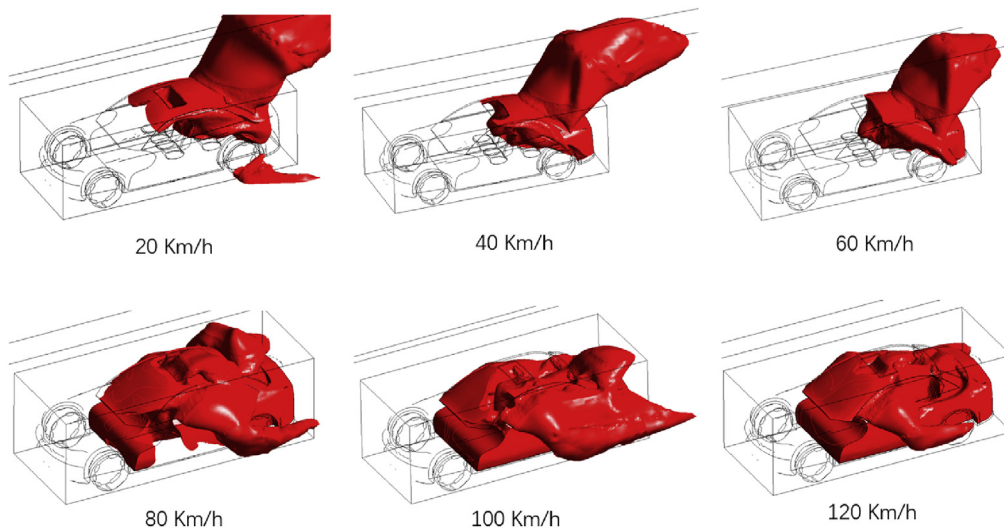
Fig. 14 — Region with flammable risk for scenarios with opened sunroof, door windows and rear windshield.

Fig. 14 presents the regions with the flammable risk for scenarios with opened sunroof, door windows and rear windshield at the same time. With the increase of wind speeds, the evolution of flammable area inside the vehicle could be divided into two different stages. When the wind speed is lower than 60 km/h, with the increase of wind speed, the area with ignition risk gradually decreases to the rear of the vehicle and the front area is safe. Thus, the size of safe region inside the vehicle is proportional to the wind speed. However, when the wind speed is higher than 80 km/h, the whole interior of the vehicle is flammable. High velocity of external air does not facilitate the dispersion of hydrogen inside the vehicle.

Conclusions

In this paper, a series of safety analysis of hydrogen leakage based on BMW Series 1 model were performed using Open-Foam. Hydrogen leaks from the pipe joint of storage tanks located in the rear of the vehicle. Different wind speeds were taken into account to investigate the influence of ambient wind. Based on numerical results of all the scenarios, the conclusions could be drawn as follows.

1) When the sunroof or door windows are opened, the distribution of hydrogen in the vehicle is strongly affected by ambient wind.
2) For scenarios with opened sunroof only, in the case of accidental leakage, hydrogen is extremely difficult to diffuse and personnel should be as far away as possible.
3) For scenarios with opened door windows only or opening door windows and sunroof both, hydrogen in the front of the vehicle could be discharged only when ambient wind speed is at around 100 km/h. When wind speed is lower than 60 km/h, hydrogen could not be discharged from the vehicle smoothly.
4) When the ambient wind speed is less than 60 km/h, the front area of the vehicle could be successfully kept away from the flammable risk by opening the sunroof, door windows and rear windshield at the same time. If hydrogen is kept away from the electronic equipment at the front part of the vehicle, the interior is relatively away from the flammable risk.

In further work, more scenarios, such as opening vehicle trunk or changing position of storage tanks, need be considered. The hydrogen discharged from the vehicle may also cause serious explosion accidents if it encounters other vehicles behind. Therefore, the influence of hydrogen fuel cell vehicles with flammable risk on other vehicles around is also necessary to be considered further.

Acknowledgement

REFERENCES

[1] https://en.wikipedia.org/wiki/Toyota_Mirai. 2018.
[2] Schefer RW HW, Moen CD, Chan JP, Maness MA, Keller JO. Hydrogen codes and standards unintended release workshop: workshop analysis., workshop held December 12, 2003. Livermore CA: Sandia National Laboratories; 2004.
[3] ISO/TR 15916:2015 Basic considerations for the safety of hydrogen systems. 2015.
[4] Middha P, Hansen OR. CFD simulation study to investigate the risk from hydrogen vehicles in tunnels. Int J Hydrogen Energy 2009;34(14):5875–86.
[5] Houf WG, Evans GH, Merilo E, Groethe M, James SC. Releases from hydrogen fuel-cell vehicles in tunnels. Int J Hydrogen Energy 2012;37(1):715–9.
[6] Choi J, Hur N, Kang S, Lee ED, Lee K-B. A CFD simulation of hydrogen dispersion for the hydrogen leakage from a fuel cell vehicle in an underground parking garage. Int J Hydrogen Energy 2013;38(19):8084–91.
[7] Kožuh M. Preventing hydrogen detonations in road tunnels hydrogen trap concept. Int J Hydrogen Energy 2014;39(30):17434–9.
[8] G. AS, FLACS user manual v9, Bergen, Norway.
[9] Liu W, Christopher DM. Dispersion of hydrogen leaking from a hydrogen fuel cell vehicle. Int J Hydrogen Energy 2015;40(46):16673–82.
[10] Tamura Y, Takeuchi M, Sato K. Effectiveness of a blower in reducing the hazard of hydrogen leaking from a hydrogen-fueled vehicle. Int J Hydrogen Energy 2014;39(35):20339–49.
[11] Salva JA, Tapia E, Iranzo A, Pino FJ, Cabrera J, Rosa F. Safety study of a hydrogen leak in a fuel cell vehicle using computational fluid dynamics. Int J Hydrogen Energy 2012;37(6):5299–306.
[12] Xu BP, Zhang JP, Wen JX, Dembele S, Karwatzki J. Numerical study of a highly under-expanded hydrogen jet. 2005.
[13] Birch AD, Brown DR, Dodson MG, Swaffield F. The structure and concentration decay of high pressure jets of natural gas. Combust Sci Technol 1984;36(5–6):249–61.
[14] Baraldi D, Papanikolaou E, Heitsch M. Gap analysis of CFD modelling of accidental hydrogen release and combustion. Luxembourg Publications Office of the European Union; 2010.
[15] HySafe. Biennal report on hydrogen safety, chapter III: accidental phenomena and consequences. 2007.
[16] Papanikolaou E, Baraldi D, Kuznetsov M, Venetsanos A. Evaluation of notional nozzle approaches for CFD simulations of free-shear under-expanded hydrogen jets. Int J Hydrogen Energy 2012;37(23):18563–74.
[17] Birch AD, Hughes DJ, Swaffield F. Velocity decay of high pressure jets. Combust Sci Technol 1987;52(1–3):161–71.
[18] Ewan BCR, Moodie K. Structure and velocity measurements in underexpanded jets. Combust Sci Technol 1986;45(5–6):275–88.
[19] Schefer RW, Houf WG, Williams TC, Bourne B, Colton J. Characterization of high-pressure, underexpanded hydrogen-jet flames. Int J Hydrogen Energy 2007;32(12):2081–93.
[20] Chenoweth DR. Gas-Transfer analysis. Section H - real gas results via the van der Waals equation of state and virial-expansion extensions of its limiting abel-nobel form. 1983.
[21] Yüceil KB, Ötügen MV. Scaling parameters for underexpanded supersonic jets. Phys Fluids 2002;14(12):4206–15.

[22] Xiao J, Travis JR, Breitung W. Hydrogen release from a high pressure gaseous hydrogen reservoir in case of a small leak. Int J Hydrogen Energy 2011;36(3):2545—54.

[23] Harstad K, Bellan J. Global analysis and parametric dependencies for potential unintended hydrogen-fuel releases. Combust Flame 2006;144(1):89—102.

[24] DB S. Combustion and mass transfer. Oxford: Pergamon Press Ltd.; 1979.

[25] Hourri A, Gomez F, Angers B, Bénard P. Computational study of horizontal subsonic free jets of hydrogen: validation and classical similarity analysis. Int J Hydrogen Energy 2011;36(24):15913—8.

[26] Chen CJ, Rodi W. Vertical turbulent buoyant jets: a review of experimental data, nasa sti/recon technical report a 80. 1980.

[27] SB P. Turbulent flows. Cambridge University Press; 2003.

[28] OpenFOAM users' guide. Available from: http://www.opencfd.co.uk/openfoam/.

[29] Hoffman MJZJD. Gas dynamics. 1976. Boston.

[30] GB/T 28591. Wind scale. 2012.